HEAT TRANSFER ANALYSIS OF MHD FLOW DUE TO UNSTEADY BI-DIRECTIONAL STRETCHING SHEET THROUGH POROUS SPACE

by

Iftikhar AHMAD[a*], Manzoor AHMAD[a], and Muhammad SAJID[b]

[a] Department of Mathematics, Azad Kashmir University, Muzaffarabad, Pakistan
[b] Theoretical Physics Division, Pakistan Institute of Nuclear Science and Technology, Nilore, Islamabad, Pakistan

Original scientific paper
DOI: 10.2298/TSCI140313114A

In this article unsteady 3-D MHD boundary layer flow and heat transfer analysis with constant temperature and constant heat flux in a porous medium is considered. The boundary layer flow is governed by a bi-directional stretching sheet. Similarity transformations are used to transform the governing non-linear partial differential equations to ordinary differential equations. Analytical solutions are constructed using homotopy analysis method. Convergence analysis is also presented through tabular data. The quantities of interest are the velocity, temperature, skin friction coefficient,t and Nusselt number. The obtained results are validated by comparisons with previously published work in special cases. The results of this parametric study are shown graphically and the physical aspects of the problem are discussed.

Key words: *porous medium, MHD, stretching, unsteady, 3-D, homotropy analysis method*

Introduction

Boundary layer flows over a moving surface have been extensively targeted by many researchers during past few decades due to their importance in engineering and industrial processes. These flows have abundant applications in many technological processes including paper productions, glass fiber, manufacturing plastic films, crystal growing, hot rolling, and many others. After the pioneering work done by Sakiadis [1, 2] on the boundary layer flow past a moving plate many investigators have discussed the various aspects of stretching phenomenon. Much attention in the past has been given to 2-D boundary layer flows over a steady stretching sheet [3-9], and abundant literature in this direction is available. All the studies previously mentioned were carried out when the sheet is stretched linearly in one direction. Wang [10] discussed 3-D flow of a viscous fluid due to the stretching of the elastic surface in two lateral directions. Heat transfer in fluid flows is an important phenomenon and for the details of fluid flow phenomena for in-tube/external forced convection the readers are referred to articles [11-15]. The present problem can be investigated through the recent developed techniques such as the use of inserts, non-uniform heating effect, geometrical optimization, the effect of wall axial conduction (conjugate case), generalized (power-law) fluid case, disturbed velocity, *etc.* [16-23].

* Corresponding author: e-mail address: aaiftikhar@yahoo.com

Heat transfer and flow through porous medium in the presence of a constant magnetic field is a phenomenon of great interest from both theoretical and practical point of view. This is due to its importance in several environmental and engineering disciplines. These applications include geothermal, petroleum resources, *in situ* combustion of oil shell, boiling enhancement using porous coatings, compact heat exchangers, packed bed reactors or absorbent, high performance of building insulation, *etc.* There is still a great deal of theoretical as well as practical interest in this area of research due to wide range of applications and importance. A glance at literature show some recent studies dealing with the MHD flow through porous medium over a stretching sheet [24-32] and references therein. Liu and Andersson [33] investigated the heat transfer characteristics over a bi-directional stretching sheet with variable thermal conditions in the presence of a temperature-dependent internal heat source (or sink). Ahmad *et al.* [34] analyzed heat transfer characteristics for 2-D flow of a steady viscous fluid over an exponentially stretching sheet with variable thermal conductivity through porous medium in the presence of an applied magnetic field. The problem investigated in [34] is different from the present problem in many ways firstly here we have considered a 3-D flow instead of 2-D flow, secondly the flow is steady in [34] while here we have assumed an unsteady flow, thirdly in [34] a variable thermal conductivity is taken into account as the constant thermal conductivity in the present case.

Few attempts regarding unsteady flow over a stretching sheet can be found through [35-39]. Much attention has not been given to the unsteady flow problems regarding bi-directional stretching. Mukhopadhyay [40] examined unsteady mixed convection flow and heat transfer over a porous stretching surface. The unsteady 3-D stagnation point flow of a viscoelastic fluid has been considered by Sashadri *et al.* [41]. Recently, Hayat *et al.* [42] studied the time dependent 3-D flow and mass transfer of an elastic viscous fluid over an unsteady bi-directional stretching sheet. Based on the previous review, it is noted that the heat transfer characteristic of 3-D unsteady MHD flow due to bi-directional unsteady stretching sheet in a porous medium has not been attempted or investigated yet to the best of our information. The purpose of this paper is to present the analytic solution of unsteady MHD flow and heat transfer over a bi-directional unsteady stretching sheet in a porous medium. The analytic series solution is developed using homotropy analysis method (HAM) [43, 44]. It is important to mention here that the same problem can be investigated by using other semi-analytical methods [45-47].

Formulation of the problem

Consider the unsteady 3-D boundary layer flow of a viscous, incompressible fluid in a porous medium due to stretching surface in a plane at $z = 0$. The surface is uniformly stretched in both x- and y-directions. Flow analysis is carried out in the presence of heat generation or absorption parameter. A constant magnetic field of strength, B_0, is applied perpendicular to the flow in the z-direction. The magnetic Reynold number is assumed small so that the induced magnetic field can be neglected. The transformed form of the equations governing the unsteady MHD flow and heat transfer analysis due to bi-directional stretching sheet with constant temperature and constant heat flux are [33]:

$$f''' + (f+g)f'' - f'^2 - A\left(f' + \frac{\eta}{2}f''\right) - (\varepsilon + M^2)f' = 0 \tag{1}$$

$$g''' + (f+g)g'' - g'^2 - A\left(g' + \frac{\eta}{2}g''\right) - (\varepsilon + M^2)g' = 0 \tag{2}$$

$$\theta'' + \Pr\,(f+g)\theta' + \Pr\,(\beta - rf' - sg')\theta - A\left(\frac{\eta}{2}\theta' - \theta\right)\Pr = 0, \ \text{(CT)} \tag{3}$$

$$\phi'' + \Pr\,(f+g)\phi' + \Pr\,(\beta - rf' - sg')\phi - A\left(\frac{\eta}{2}\phi' - \phi\right)\Pr = 0, \ \text{(CH)} \tag{4}$$

subject to the boundary conditions:

$$f = 0, \quad g = 0, \quad g' = \alpha, \quad \theta = 1, \quad \phi' = -1, \quad \text{at } \eta = 0,$$
$$f' \to 0, \quad g' \to 0, \quad \theta \to 0, \quad \phi \to 0, \quad \text{as} \quad \eta \to \infty \tag{5}$$

where the prime denotes differentiation with respect to η, $\alpha = b/a$ is the stretching ratio, $A = c/a$ – the unsteadiness parameter, $\varepsilon = \phi_1/\rho a k_1$ – the porosity parameter, $M = \sigma B_0^2/a\rho$ – the magnetic parameter, $\Pr = \nu/k$ the Prandtl number, and $\beta = Q/\rho C_p a$ – the internal heat parameter.

The physical quantities of interest are the skin friction coefficients C_{fx} and C_{fy} along the x- and y-directions, respectively, and are given by:

$$C_{fx} = \frac{\tau_{wx}}{\rho u_w^2}, \qquad C_{fy} = \frac{\tau_{wy}}{\rho u_w^2} \tag{6}$$

where τ_{wx} and τ_{wy} are the wall shear stress along x- and y-directions, respectively. In dimensionless form we get:

$$\mathrm{Re}_x^{1/2}\, C_{fx} = f''(0), \qquad \mathrm{Re}_x^{1/2}\, C_{fy} = \frac{v_w}{u_w} g''(0) \tag{7}$$

where $\mathrm{Re}_x = u_w x/\nu$ is the local Reynolds number. Whe can obtain the flow equations for the steady case discussed in [9] when $A = 0$, as follows:

$$f''' + (f+g)f'' - f'^2 - (\varepsilon + M^2)f' = 0 \tag{8}$$

$$g''' + (f+g)g'' - g'^2 - (\varepsilon + M^2)g' = 0 \tag{9}$$

$$\theta'' + \Pr\,(f+g)\theta' + \Pr\,(\beta - rf' - sg')\theta = 0 \tag{10}$$

$$\phi'' + \Pr\,(f+g)\phi' + \Pr\,(\beta - rf' - sg')\phi = 0 \tag{11}$$

and the boundary conditions are given in eq. (14) of [9].

The HAM solutions

Based on the rules of solution expressions and the boundary conditions, eq. (5), the initial approximations $f_0(\eta)$, $g_0(\eta)$, $\theta_0(\eta)$, and $\phi_0(\eta)$ for the functions $f(\eta)$, $g(\eta)$, $\theta(\eta)$, and $\phi(\eta)$ are:

$$f_0(\eta) = 1 - \exp(-\eta) \tag{12}$$

$$g_0(\eta) = \alpha[1 + \exp(-\eta)] \tag{13}$$

$$\theta_0(\eta) = \exp(-\eta) \tag{14}$$

$$\phi_0(\eta) = \exp(-\eta) \tag{15}$$

and the auxiliary linear operators are:

$$\mathcal{L}_1(f) = \frac{d^3 f}{d\eta^3} - \frac{df}{d\eta} \tag{16}$$

$$\mathcal{L}_2(f) = \frac{d^2 f}{d\eta^2} - f \tag{17}$$

satisfying

$$\mathcal{L}_1\left[C_1 + C_2\exp(\eta) + C_3\exp(-\eta)\right] = 0 \tag{18}$$

$$\mathcal{L}_2\left[C_4\exp(\eta) + C_5\exp(-\eta)\right] = 0 \tag{19}$$

in which C_i ($i = 1, 2, \ldots, 5$) are the arbitrary constants. From eqs. (1)-(4), the non-linear operators $\mathcal{N}_f$, $\mathcal{N}_g$, $\mathcal{N}_\theta$, and $\mathcal{N}_\phi$ are defined:

$$\mathcal{N}_f[\hat{f}(\eta, p), \hat{g}(\eta, p)] = \frac{\partial^3 \hat{f}(\eta, p)}{\partial \eta^3} - (\varepsilon + M^2)\frac{\partial \hat{f}(\eta, p)}{\partial \eta} - \left[\frac{\partial \hat{f}(\eta, p)}{\partial \eta}\right]^2 + \\ + [\hat{f}(\eta, p) + \hat{g}(\eta, p)]\frac{\partial^2 \hat{f}(\eta, p)}{\partial \eta^2} - A\left[\frac{\eta}{2}\frac{\partial^2 \hat{f}(\eta, p)}{\partial \eta^2} + \frac{\partial \hat{f}(\eta, p)}{\partial \eta}\right] \tag{20}$$

$$\mathcal{N}_g[\hat{f}(\eta, p), \hat{g}(\eta, p)] = \frac{\partial^3 \hat{g}(\eta, p)}{\partial \eta^3} - (\varepsilon + M^2)\frac{\partial \hat{g}(\eta, p)}{\partial \eta} - \left[\frac{\partial \hat{g}(\eta, p)}{\partial \eta}\right]^2 + \\ + [\hat{f}(\eta, p) + \hat{g}(\eta, p)]\frac{\partial^2 \hat{g}(\eta, p)}{\partial \eta^2} - A\left[\frac{\eta}{2}\frac{\partial^2 \hat{g}(\eta, p)}{\partial \eta^2} + \frac{\partial \hat{g}(\eta, p)}{\partial \eta}\right] \tag{21}$$

$$\mathcal{N}_\theta[\hat{f}(\eta, p), \hat{g}(\eta, p)] = \frac{\partial^2 \hat{\theta}(\eta, p)}{\partial \eta^2} + \Pr[\hat{f}(\eta, p) + \hat{g}(\eta, p)]\frac{\partial \hat{\theta}(\eta, p)}{\partial \eta} + \\ + \Pr\left[\beta - r\frac{\partial \hat{f}(\eta, p)}{\partial \eta} - s\frac{\partial \hat{g}(\eta, p)}{\partial \eta}\right]\hat{\theta}(\eta, p) - A\left[\frac{\eta}{2}\frac{\partial \hat{\theta}(\eta, p)}{\partial \eta} + \hat{\theta}(\eta, p)\right]\Pr \tag{22}$$

$$\mathcal{N}_\phi[\hat{f}(\eta, p), \hat{g}(\eta, p)] = \frac{\partial^2 \hat{\phi}(\eta, p)}{\partial \eta^2} + \Pr[\hat{f}(\eta, p) + \hat{g}(\eta, p)]\frac{\partial \hat{\phi}(\eta, p)}{\partial \eta} + \\ + \Pr\left[\beta - r\frac{\partial \hat{f}(\eta, p)}{\partial \eta} - s\frac{\partial \hat{g}(\eta, p)}{\partial \eta}\right]\hat{\phi}(\eta, p) - A\left[\frac{\eta}{2}\frac{\partial \hat{\phi}(\eta, p)}{\partial \eta} + \hat{\phi}(\eta, p)\right]\Pr \tag{23}$$

If $p \in [0, 1]$ is the embedding parameter, and $\hbar_f$, $\hbar_g$, $\hbar_\theta$, and $\hbar_\phi$, are the non-zero auxiliary parameters, the 0$^{\text{th}}$-order deformation problems are of the following form:

$$(1 - p)\mathcal{L}_1[\hat{f}(\eta, p) - f_0(\eta)] = p\hbar_f \mathcal{N}_f[\hat{f}(\eta, p), \hat{g}(\eta, p)] \tag{24}$$

$$(1 - p)\mathcal{L}_1[g(\eta, p) - g_0(\eta)] = p\hbar_g \mathcal{N}_g[\hat{f}(\eta, p), \hat{g}(\eta, p)] \tag{25}$$

$$(1-p)\mathcal{L}_2[\hat{\theta}(\eta,\, p)-\theta_0(\eta)] = p\hbar_\theta \mathcal{N}_\theta[\hat{f}(\eta,\, p)+\hat{g}(\eta,\, p)] \tag{26}$$

$$(1-p)\mathcal{L}_2[\hat{\phi}(\eta,\, p)-\phi_0(\eta)] = p\hbar_\phi \mathcal{N}_\phi[\hat{f}(\eta,\, p)+\hat{g}(\eta,\, p)] \tag{27}$$

$$\hat{f}(0,\, p) = \hat{g}(0,\, p) = 0, \qquad \left.\frac{\partial \hat{f}(\eta,\, p)}{\partial \eta}\right|_{\eta=0} = \hat{\theta}(0,\, p) = 1,$$
$$\left.\frac{\partial \hat{g}(\eta,\, p)}{\partial \eta}\right|_{\eta=0} = \alpha\,, \qquad \left.\frac{\partial \hat{\phi}(\eta,\, p)}{\partial \eta}\right|_{\eta=0} = -1 \tag{28}$$

$$\left.\frac{\partial \hat{f}(\eta,\, p)}{\partial \eta}\right|_{\eta=+\infty} = \left.\frac{\partial \hat{g}(\eta,\, p)}{\partial \eta}\right|_{\eta=+\infty} = \hat{\theta}(\infty,\, p) = \hat{\phi}(\infty,\, p) = 0 \tag{29}$$

Previous equations clearly imply that for $p = 0$ and $p = 1$ these have the following solutions:

$$\hat{f}(\eta,\, 0) = f_0(\eta), \qquad \hat{f}(\eta, 1) = f(\eta) \tag{30}$$

$$\hat{g}(\eta,\, 0) = g_0(\eta), \qquad \hat{g}(\eta, 1) = g(\eta) \tag{31}$$

$$\hat{\theta}(\eta,\, 0) = \theta_0(\eta), \qquad \hat{\theta}(\eta, 1) = \theta(\eta) \tag{32}$$

$$\hat{\phi}(\eta,\, 0) = \phi_0(\eta), \qquad \hat{\phi}(\eta, 1) = \phi(\eta) \tag{33}$$

As p increase from 0 to 1 continuously, $\hat{f}(\eta,\, p)$, $\hat{g}(\eta,\, p)$, $\hat{\theta}(\eta,\, p)$, and $\hat{\phi}(\eta,\, p)$ vary from $f_0(\eta)$, $g_0(\eta)$, $\theta_0(\eta)$, and $\phi_0(\eta)$ to the solutions $f(\eta)$, $g(\eta)$, $\theta(\eta)$, and $\phi(\eta)$. The Taylor's series thus suggest that:

$$\hat{f}(\eta,\, p) = f_0(\eta) + \sum_{m=1}^{\infty} f_m(\eta) p^m, \qquad f_m(\eta) = \frac{1}{m\,!} \left.\frac{\partial^m \hat{f}(\eta,\, p)}{\partial p^m}\right|_{p=0} \tag{34}$$

$$\hat{g}(\eta,\, p) = g_0(\eta) + \sum_{m=1}^{\infty} g_m(\eta) p^m, \qquad g_m(\eta) = \frac{1}{m\,!} \left.\frac{\partial^m \hat{g}(\eta,\, p)}{\partial p^m}\right|_{p=0} \tag{35}$$

$$\hat{\theta}(\eta,\, p) = \theta_0(\eta) + \sum_{m=1}^{\infty} \theta_m(\eta) p^m, \qquad \theta_m(\eta) = \frac{1}{m\,!} \left.\frac{\partial^m \theta(\eta,\, p)}{\partial p^m}\right|_{p=0} \tag{36}$$

$$\hat{\phi}(\eta,\, p) = \phi_0(\eta) + \sum_{m=1}^{\infty} \phi_m(\eta) p^m, \qquad \phi_m(\eta) = \frac{1}{m\,!} \left.\frac{\partial^m \phi(\eta,\, p)}{\partial p^m}\right|_{p=0} \tag{37}$$

The convergence of previous series depend upon the auxiliary parameters $\hbar_f$, $\hbar_g$, $\hbar_\theta$, and $\hbar_\phi$. Assuming that $\hbar_f$, $\hbar_g$, $\hbar_\theta$, and $\hbar_\phi$, are chosen such that the series in eqs. (34)-(37) are convergent at $p = 1$. Therefore:

$$f(\eta) = f_0(\eta) + \sum_{m=1}^{\infty} f_m(\eta) \tag{38}$$

$$g(\eta) = g_0(\eta) + \sum_{m=1}^{\infty} g_m(\eta) \tag{39}$$

$$\theta(\eta) = \theta_0(\eta) + \sum_{m=1}^{\infty} \theta_m(\eta) \tag{40}$$

$$\phi(\eta) = \phi_0(\eta) + \sum_{m=1}^{\infty} \phi_m(\eta) \tag{41}$$

Equations (38)-(41) have the general solutions in the form:

$$f_m(\eta) = f_m^*(\eta) + C_1 + C_2 \exp(\eta) + C_3 \exp(-\eta) \tag{42}$$

$$g_m(\eta) = g_m^*(\eta) + C_4 + C_5 \exp(\eta) + C_6 \exp(-\eta) \tag{43}$$

$$\theta_m(\eta) = \theta_m^*(\eta) + C_7 \exp(\eta) + C_8 \exp(-\eta) \tag{44}$$

$$\phi_m(\eta) = \phi_m^*(\eta) + C_9 \exp(\eta) + C_{10} \exp(-\eta) \tag{45}$$

where $f_m^*(\eta)$, $g_m^*(\eta)$, $\theta_m^*(\eta)$, and $\phi_m^*(\eta)$ denote the special solutions.

Convergence of the HAM solutions

The series solutions given in eqs. (38)-(41) contain the auxiliary parameters $\hbar_f$, $\hbar_g$, $\hbar_\theta$, and $\hbar_\phi$. As pointed out by Liao [43, 44], the rate of approximation and the convergence of the solutions strongly depends upon the values of $\hbar_f$, $\hbar_g$, $\hbar_\theta$, and $\hbar_\phi$. In the present case the proper values of $\hbar_f$, $\hbar_g$, $\hbar_\theta$, and $\hbar_\phi$ are chosen through $\hbar$-curves of $f''(0)$, $g''(0)$, $\theta'(0)$, and $\phi'(0)$ for 15th-order of approximation in fig. 1. The $\hbar$-curves suggest that we can take $\hbar_f = \hbar_g = \hbar_\theta = \hbar_\phi = \hbar$, and thus the range of the admissible values of $\hbar$ is $-1.15 \le \hbar \le 0.25$.

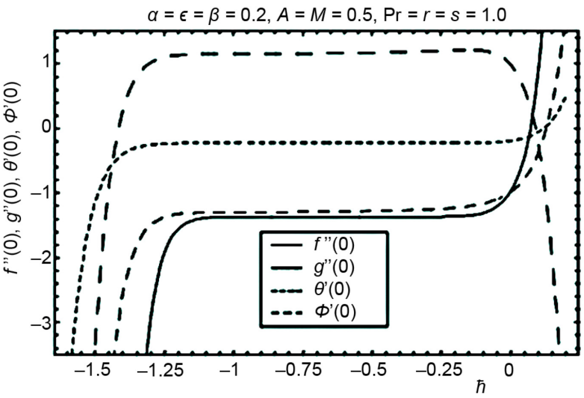

Figure 1. The $\hbar$-curves for $f''(0)$, $g''(0)$, $\theta'(0)$, and $\phi'(0)$ at 15th-order of approximation

Table 1 has been prepared to see how many orders of approximations are required for obtaining a convergent solution up to six decimal places. The results show that for velocities f and g a 12th order solution is sufficient however for θ and ϕ the required convergence will be achieved at 35th order solution.

Results and discussion

The HAM solutions in the form of an infinite series are obtained using symbolic software MATHEMATICA. The values of $\hbar$ are chosen in such a way that the obtained series is convergent for the chosen set of fluid parameters appearing in the problem. In the present discussion we are only focusing on the discussion of temperature profile and heat transfer across the surface for both constant surface temperature and constant heat flux cases. To depict the

Table 1. Numerical values of $f''(0)$, $g''(0)$, $\theta'(0)$, and $\phi''(0)$ at different order of approximations when $\alpha = M = A = 0.5$, $\varepsilon = \beta = 0.2$, $\Pr = r = s = 1.0$, and $\hbar = -0.7$

Order of approximation	$-f''(0)$	$-g''(0)$	$-\theta'(0)$	$-\phi'(0)$
1	1.347083	0.615208	1.294444	1.505556
5	1.410516	0.642890	1.401450	1.280844
10	1.410840	0.643027	1.428101	1.258486
12	1.410840	0.643028	1.432944	1.254651
15	1.410840	0.643028	1.437704	1.250936
20	1.410840	0.643028	1.442124	1.247541
25	1.410840	0.643028	1.444405	1.245815
30	1.410840	0.643028	1.445654	1.244882
35	1.410840	0.643028	1.446355	1.244366
40	1.410840	0.643028	1.446355	1.244366

influence of different parameters on the temperature profiles figs. 2-9 have been plotted. In all figs. 2-9, on 2(a), is referred to the constant surface temperature (CT) case and 9(b), is referred to constant heat (CH) flux case. The influence of parameter A on temperature profiles θ and ϕ for 3-D flow situation is portrayed in fig. 2.

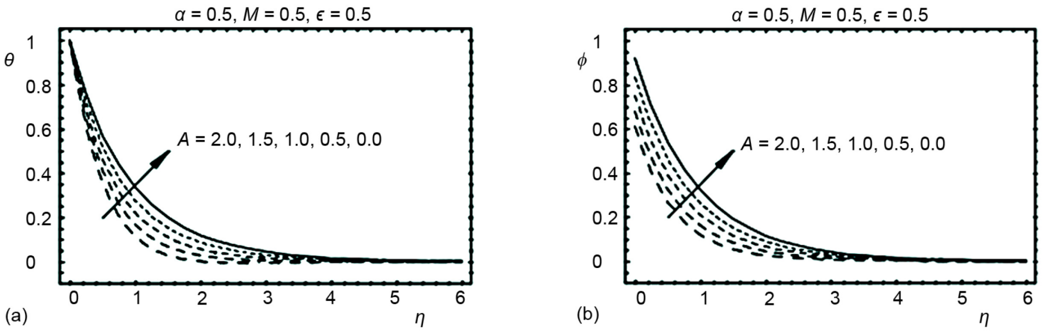

Figure 2. Influence of unsteadiness parameter A on temperature; (a) CT case, (b) CH case

This figure shows that temperature is a decreasing function of A for both CT and CH cases. It is also noted that the thermal boundary layer decreases with an increase in A. Figure 3 describe the effect of porosity parameter on the temperature profiles. It is evident from these figures that the temperature is high when fluid is passing through a porous medium. Figure 4 shows the effects of the magnetic parameter, M, on the dimensionless temperature profiles. The temperature increases by increasing the values of the magnetic parameter in both the cases of CT and flux CH, respectively. Figure 5 elucidates the influences of the stretching ratio, α, on the temperature profiles. It is observed that the temperature profile decreases with increasing values of the stretching ratio in both CT and CH cases. It is also observed that the thermal boundary layer is decreased for large values of the stretching ratio. It is further noted that these results are in qualitatively similar with the temperature profiles shown by Liu and Andersson [33] in the presence of the magnetic field and porous medium. The impact of power index r and s on the temperature profiles is seen through figs. 6 and 7. It is observed that both the indices have similar effect on the temperature profiles. The r and s decreases the temperature and thermal boundary layer thickness. Figure 8 shows the effects of the heat source/sink parameter, β, on the temperatures θ and ϕ. As expected, the temperature increases with increasing heat source $\beta > 0$, and decreases in the case of heat sink $\beta < 0$. The behavior of Prandtl number, is same is as that of unsteadiness parameter A as shown in fig. 9.

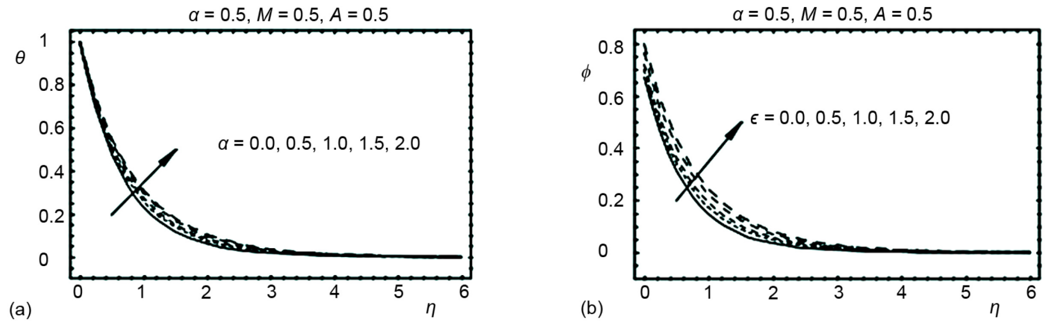

Figure 3. Influence of porosity parameter ε on temperature; (a) CT case, (b) CH case

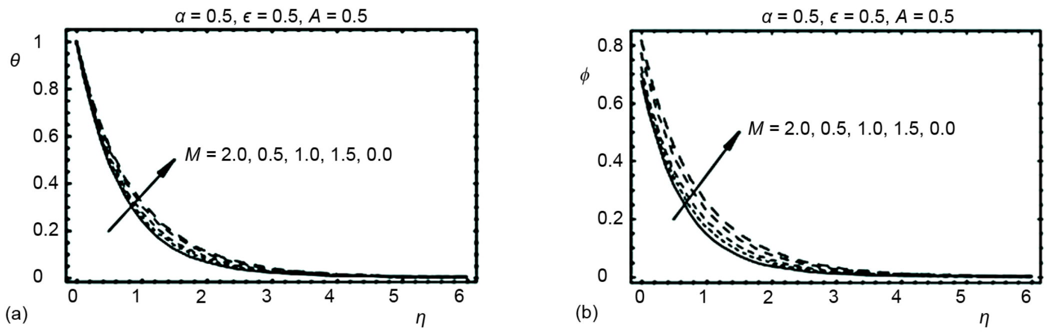

Figure 4. Influence of magnetic parameter M on temperature; (a) CT case, (b) CH case

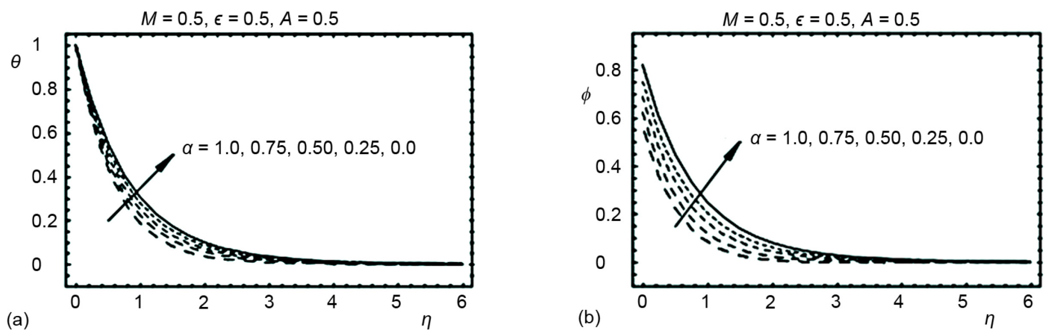

Figure 5. Influence of stretching parameter α on temperature; (a) CT case, (b) CH case

Table 2 shows the values of the heat transfer rate at the surface $\theta'(0)$ for different values of r and s with $\beta = 0$, and Pr = 1 in the case of $M = \varepsilon = A = 0$. It is found that the temperature gradient at the surface $\theta'(0)$ becomes positive and decreases for $r = -2$ and $s = 0$, and

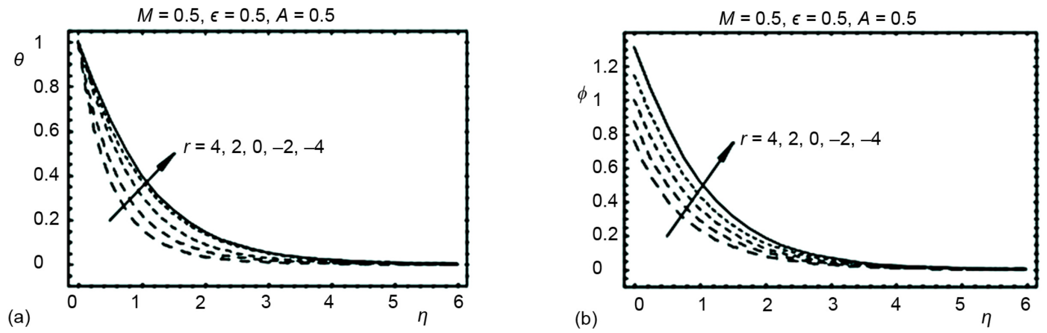

Figure 6. Influence of *r* on temperature (a) CT case, (b) CH case

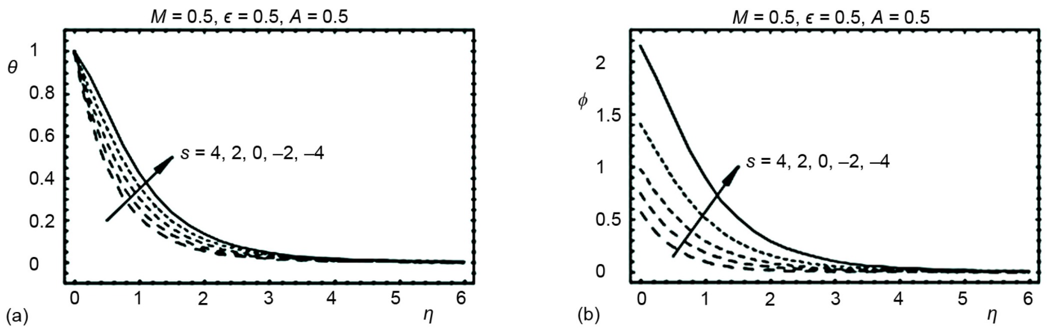

Figure 7. Influence of *s* on temperature; (a) CT case, (b) CH case

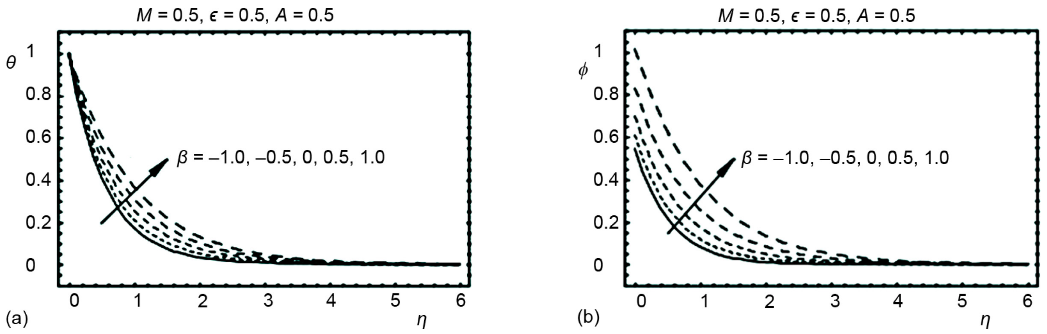

Figure 8. Influence of *β* on temperature; (a) CT case, (b) CH case

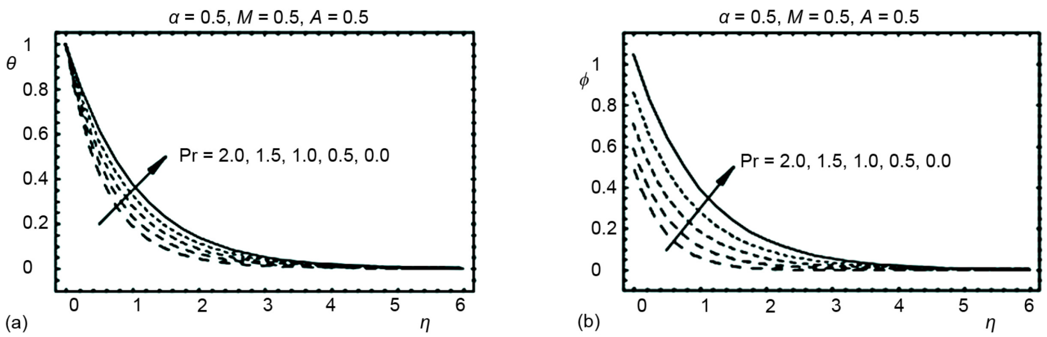

Figure 9. Influence of Prandtl number on temperature; (a) CT case, (b) CH case

Table 2. Numerical values of $\theta'(0)$, when Pr = 1, β = 0, and $\varepsilon = M = 0 = A$

	$r = 0, s = 0$	$r = -2, s = 0$	$r = 2, s = 0$	$r = 0, s = -2$	$r = 0, s = 2$
$\alpha = 0.25$ [36] Present solution	–0.665933 –0.665927	0.554512 0.554573	–1.364890 –1.364890	–0.413111 –0.413101	–0.883125 –0.883123
$\alpha = 0.50$ [36] Present solution	–0.735334 –0.735333	0.308578 0.308590	–1.395356 –1.395357	–0.263381 –0.263376	–1.106491 –1.106500
$\alpha = 0.75$ [36] Present solution	–0.796472 –0.796470	0.135471 0.135470	–1.425038 –1.425037	–0.126679 –0.126680	–1.292003 –1.292010

Table 3. Numerical values of $\theta'(0)$ with β = 0, ε =0.2, M = 0.5, A = 0.5, and Pr = 1

	$r = 0, s = 0$	$r = -2, s = 0$	$r = 2, s = 0$	$r = 0, s = -2$	$r = 0, s = 2$
$\alpha = 0.25$	–1.06877	–0.35239	–1.60771	–0.90357	–1.22165
$\alpha = 0.50$	–1.12062	–0.44678	–1.64075	–0.80250	–1.40153
$\alpha = 0.75$	–1.16969	–0.53416	–1.67353	–0.70587	–1.55989

negative for $r = 0$ and $s = -2$. It is noted that the present results obtained by agree well with the numerical results of Liu and Andersson [33]. Table 3 gives the values of $\theta'(0)$ for different values of r and s with $\beta = 0$, and Pr = 1 in the presence of magnetic field $M = 0.5$ and the porosity parameter $\varepsilon = 0.2$. It is observed that the temperature gradient at the surface $\theta'(0)$ has the same behavior in case of $M = 0.5$, $A = 0.5$, and $\varepsilon = 0.2$, but its magnitude is smaller in this case when compared with the case of $M = \varepsilon = A = 0$.

Table 4 give the numerical values of the temperature gradient at the surface $\theta'(0)$ and $\phi(0)$ for different values of Prandtl number and β with $\alpha = 0.5$, $s = 1$, $r = 1$, and $M = \varepsilon = 0$. The magnitude of the temperature gradient at the surface $\theta'(0)$ increases by increasing the values of Prandtl number and $-\theta'(0)$ reduces with the increasing values of β. It is also noted from this table that in the case of prescribed surface heat flux at the sheet, a heat source (sink) tends to reduce the sheet temperature $\phi(0)$. Table 5 shows the numerical values of temperature gradient at the surface $\theta'(0)$ and $\phi(0)$ for different values of Prandtl number and $\beta = 0$ with $\alpha = 0.5$, $s = 1$, and $r = 1$ in the case of $M = 0.5$, $A = 0.5$, and $\varepsilon = 0.2$. It is noted that the magnitude of the temperature gradient at the surface $\theta'(0)$ is smaller, whereas the sheet temperature $\phi(0)$ in case of CH flux at the sheet is larger quantitatively in the presence of magnetic field $M = 0.5$ and the porosity parameter $\varepsilon = 0.2$.

Table 4. Numerical values of $\theta'(0)$ and $\phi(0)$, when ε =0, M = 0, A = 0, r = 1.0, s = 1, and α = 0.5

		$\theta'(0)$ for CT			$\phi(0)$ for CH		
		$\beta = -0.2$	$\beta = 0$	$\beta = 0.2$	$\beta = -0.2$	$\beta = 0$	$\beta = 0.2$
Ref. [36] Present	Pr = 1	–1.348064 –1.348067	–1.255781 –1.255779	–1.148932 –1.148935	0.741805 0.741807	0.796317 0.796319	0.870355 0.870373
Ref. [36] Present	Pr = 5	–3.330392 –3.330397	–3.170979 –3.170983	–3.002380 –3.002383	0.300265 0.300257	0.315360 0.315365	0.333069 0.333073
Ref. [36] Present	Pr =10	–4.812149 –4.812153	–4.597141 –4.597145	–4.371512 –4.371517	0.207807 0.207808	0.217527 0.217530	0.228754 0.228757

Table 5. Numerical values of $\theta'(0)$ and $\phi(0)$, when ε =0.2, M = 0.5, r = 1.0, s = 1, and α = 0.5

	$\theta'(0)$ for CT			$\phi(0)$ for CH		
	β = –0.2	β = 0	β = 0.2	β = –0.2	β = 0	β = 0.2
Pr = 1	–1.59799	–1.52437	–1.44499	0.625740	0.655917	0.691826
Pr = 5	–4.09759	–3.90322	–3.65098	0.242678	0.251869	0.263572
Pr = 10	–5.80320	–5.79601	–6.02739	0.162425	0.168834	0.176355

Concluding remarks

The MHD 3-D flow and heat transfer characteristics of a viscous fluid due to an unsteady bi-directional stretching sheet through a porous medium is investigated in this paper. For the heat transfer analysis the heating process of CT, and CH are taken into account. The influence of the various parameters of interest is analyzed through similarity solution of the governing equations. The convergence of the developed series solution is explicitly discussed. A comparison with the existing results in the literature is also made and found in excellent agreement.

Nomenclature

A – unsteadiness parameter
a, b, c – stretching constant [T^{-1}]
B_0 – magnetic field strength
C_1-C_{10} – integration constants
C_{fx} – skin friction coefficient in x-direction
C_{fy} – skin friction coefficient in y-direction
C_p – specific heat
f, g – dimensionless velocities
k – thermal conductivity
k_1 – permeability of the medium
M – magnetic parameter
Pr – Prandtl number
p – embedding parameter
Q – heat source or sink
r, s – power indices
x, y, z – Cartesian co-ordinates

Greek symbols

α – stretching ratio
β – internal heat parameter
ε – porosity parameter
η – dimensionless independent co-ordinate
θ, ϕ – dimensionless temperatures
ν – kinematic viscosity
ρ – fluid density
σ – electrical conductivity
ϕ_1 – porosity of the medium

Other symbols

$\hbar_f$, $\hbar_g$, $\hbar_\theta$, $\hbar_\phi$ – auxiliary parameters

Acknowledgment

The authors are grateful to the anonymous reviewer for his valuable comments which helps us in improving the manuscript a lot. Author acknowledges the support provided by HEC and ICTP.

References

[1] Sakiadis, B. C., Boundary Layer Behavior on Continuous Solid Surface. I. Boundary Layer Equation for Two-Dimensional and Axisymmetric Flow, *AIChE J., 7* (1961), 1, pp. 26-28
[2] Sakiadis, B. C., Boundary Layer Behavior on Continuous Solid Surface. II. Boundary Layer Equations on Continuous Solid Surface, *AIChE J., 7* (1961), 2, pp. 221-225
[3] McCormack, P. D., Crane, L., *Physical Fluid Dynamics,* Academic press, New York, USA, 1973
[4] Vleggaar, J., Laminar Boundary Layer Behaviour on Continuous Accelerating Surface, *Chem. Eng. Sci., 32* (1977), 12, pp. 1517-1525
[5] Magyari, E., Keller, B., Exact Solutions for Self-Similar Boundary-Layer Flows Induced by Permeable Stretching Walls, *Eur. J. Mech. B-Fluids, 19* (2000), 1, pp. 109-122

[6] Crane, L., Flow Past a Stretching Plate, *Z. Angew. Math. Mech. 21* (1970), 4, pp. 645-647
[7] Banks, W. H. H., Similarity Solutions of the Boundary Layer Equations for a Stretching Wall, *J. Mech. Theor. Appl., 2* (1983), 3, pp. 375-392
[8] Abbasbandy, S., The Application of Homotopy Analysis Method to Non-Linear Equation Arising in Heat Transfer, *Phys. Lett. A, 360* (2006), 1, pp. 109-113
[9] Ahmad I., *et al.,* Hydromagnetic Flow and Heat Transfer over a Bi-Directional Stretching Surface in a Porous Medium, *Thermal Sciences, 15* (2011), Suppl. 2, pp. S205-S220
[10] Wang, C. Y., The Three Dimensional Flow Due to Stretching Surface, *Phys. Fluids, 27* (1984), 8, pp. 1915-1917
[11] Ko, T. H., Ting, K., Optimal Reynolds Number for the Fully Developed Laminar Forced Convection in a Helical Coiled Tube, *Energy, 31* (2006), 12, pp. 2142-2152
[12] Hajmohammadi, M. R., *et al*., A New Configuration of Bend Tubes for Compound Optimization of Heat and Fluid Flow, *Energy 62* (2013), Dec., pp. 418-424
[13] Hajmohammadi, M. R., *et al*., Detailed Analysis for the Cooling Performance Enhancement of a Heat Source under a Thick Plate, *Ener. Con. Manag. 76* (2013), Dec., pp. 691-700
[14] Jiang, L., *et al*., Thermal Performance of a Novel Porous Crack Composite Wick Heat Pipe, *Ener. Con. Manag. 81* (2014), May, pp. 10-18
[15] Hajmohammadi, M. R., *et al*., Effect of a Thick Plate on the Excess Temperature of Iso-Heat Flux Heat Sources Cooled by Laminar Forced Convection Flow; Conjugate Analysis, *Numer. Heat Transf. A 66* (2014), 2, pp. 205-216
[16] Lesage, F. J., *et al.*, A Study on Heat Transfer Enhancement Using Flow Channel Inserts for Thermoelectric Power Generation, *Ener. Con. Manag. 75* (2013), Nov., pp. 532-541
[17] Wang, J., *et al.,* Heat Transfer Enhancement through Control of Added Perturbation Velocity in Flow Field, *Ener. Con. Manag. 70* (2013), June, pp. 194-201
[18] Pouzesh, A., *et al.*, Investigations on the Internal Shape of Constructal Cavities Intruding a Heat Generating Body, *Thermal Science, 19* (2015), 2, pp. 609-618
[19] Hajmohammadi, M. R., *et al*., New Methods to Cope with Temperature Elevations in Heated Segments of Flat Plates Cooled by Boundary Layer Flow, *Thermal Science, 20* (2016), 1, pp. 45-52
[20] Hajmohammadi, M. R., *et al*., Optimal Design of Unequal Heat Flux Elements for Optimized Heat Transfer Inside a Rectangular Duct, *Energy, 68* (2014), Apr., pp. 609-616
[21] Hajmohammadi, M. R., *et al*., Improvement of Forced Convection Cooling Due to the Attachment of Heat Sources to a Conducting Thick Plate, *ASME J. Heat Transf., 135* (2013), 12, 124504
[22] Hajmohammadi, M. R., Nourazar, S. S., Conjugate Forced Convection Heat Transfer from a Heated Flat Plate of Finite Thickness and Temperature-Dependent Thermal Conductivity, *Heat Transf. Eng., 35* (2014), 9, pp. 863-874
[23] Hajmohammadi, M. R., Nourazar, S. S., On the Insertion of a Thin Gas Layer in Micro Cylindrical Couette Flows Involving Power-Law Liquids, *Int. J. Heat Mass Transf., 75* (2014), Avg., pp. 97-108
[24] Dessie, H., Kishan, N., MHD Effects on Heat Transfer over Stretching Sheet Embedded in Porous Medium with Variable Viscosity, Viscous Dissipation and Heat Source/Sink, *Ain Shams Eng. J., 5* (2014), 3, pp. 967-977
[25] Rashad, A. M., Effects of Radiation and Variable Viscosity on Unsteady MHD Flow of a Rotating Fluid from Stretching Surface in Porous Medium, *J. Egyp. Math. Soc., 22* (2014), 1, pp. 134-142
[26] Nadeem, S., *et al.*, MHD Three-Dimensional Casson Fluid Flow past a Porous Linearly Stretching Sheet, *Alex. Eng. J., 52* (2013), 4, pp. 577-582
[27] Pahlavan, A. A., *et al*., MHD Flows of UCM Fluids above Porous Stretching Sheets Using Two-Auxiliary-Parameter Homotopy Analysis Method, *Commun. Nonlinear Sci. Numer. Simul., 14* (2009), 2, pp. 473-488
[28] Aly, E. H., Vajravelu, K., Exact and Numerical Solutions of MHD Nano Boundary-Layer Flows over Stretching Surfaces in a Porous Medium, *Appl. Math. Comput., 232* (2014), Apr., pp. 191-204
[29] Cortell, R., MHD Flow and Mass Transfer of an Electrically Conducting Fluid of Second Grade in a Porous Medium over a Stretching Sheet with Chemically Reactive Species, *Chem. Eng. Proces.: Process Intensification, 46* (2007), 8, pp. 721-728
[30] Turkyilmazoglu, M., The Analytical Solution of Mixed Convection Heat Transfer and Fluid Flow of a MHD Viscoelastic Fluid over a Permeable Stretching Surface, *Int. J. Mech. Sci., 77* (2013), Dec., pp. 263-268

[31] Ariel, P. D., Generalized Three Dimensional Flow Due to Stretching Surface, *Z. Angew. Math. Mech., 83* (2003), 12, pp. 844-852
[32] Abdullah, I. A., Analytic Solution of Heat and Mass Transfer over a Permeable Stretching Plate, *Thermal Science, 13* (2009), 2, pp. 183-197
[33] Liu, I. C, Andersson, H. I., Heat Transfer over a Bi-Directional Stretching Sheet with Variable Thermal Conditions, *Int. J. Heat Mass Transfer, 51* (2008), 15, pp. 4018-4024
[34] Ahmad, I, *et al.,* MHD Flow of a Viscous Fluid over an Exponentially Stretching Sheet in a Porous Medium, *J. Appl. Math., 2014* (2014), ID 256761
[35] Nazar, R., *et al*., Unsteady Boundary Layer Flow due to Stretching Surface in a Rotating Fluid, *Mech. Res. Commun., 31* (2009), 1, pp. 121-128
[36] Liao, S. J., An Analytic Solution of Unsteady Boundary Layer Flows Caused by an Impulsively Stretching Plate, *Commun. Non-linear Sci, Num. Simulation, 11* (2006), 3, pp. 326-339
[37] Hayat, T., *et al*., Unsteady Flow with Heat and Mass Transfer of a Third Grade Fluid over a Stretching Surface in the Presence of Chemical Reaction, *Non Linear Analysis Real World Application, 11* (2010), 4, pp. 3186-3199
[38] Elbashbeshy, E. M. A., Basid, M. A. A., Heat Transfer over an Unsteady Stretching Surface, *Heat and Mass Transfer, 41* (2004), 1, pp. 1-4
[39] Ahmad, I., On Unsteady Boundary Layer Flow of a Second Grade Fluid over a Stretching Sheet, *Add. Theor. Appl. Mech., 6* (2013), 2, pp. 95-105
[40] Mukhopadhyay, S., Effect of Thermal Radiation on Unsteady Mixed Convection Flow and Heat Transfer over a Porous Medium, *Int. J. Heat Mass Transf., 52* (2009), 13, pp. 3261-3265
[41] Seshadri, R., *et al.,* Unsteady Three Dimensional Stagnation Point Flow of a Viscoelastic Fluid, *Int. J. Eng. Sci., 35* (1997), 5, pp. 445-454
[42] Hayat, T., *et al*., Time Dependent Three Dimensional Flow and Mass Transfer of Elastico-Viscous Fluid over Unsteady Stretching Sheet, *App. Math. Mech., 32* (2011), 2, pp. 167-178
[43] Liao, S. J., The Proposed Homotopy Analysis Method for the Solution of Non-Linear Problems, Ph. D. thesis, Shangai Jiao Tong University, Shangai, China, 1992
[44] Liao, S. J., *Beyond Perturbation: Introduction to Homotopy Analysis Method*, Chapman & Hall, CRC Press, Boca Raton, Fla., USA, 2003
[45] Hajmohammadi, M. R., *et al.*, Semi-Analytical Treatment of Conjugate Heat Transfer, *J. Mech. Enging. Sci., 227* (2012), 3, pp. 492-503
[46] Hajmohammadi, M. R., Nourazar, S. S., On the Solution of Characteristic Value Problems Arising in Linear Stability Analysis; Semi Analytical Approach, *App. Math. Comp., 239* (2014), July, pp. 126-132
[47] Wazwaz, A. M., The Combined Laplace Transform – Adomian Decomposition Method for Handling Nonlinear Volterra Integro-Differential Equations, *Appl. Math. Comp., 216* (2010), 4, pp. 1304-1309

Paper submitted: March 13, 2015
Paper revised: July 16, 2015
Paper accepted: July 29, 2015